Visnyk NTUU KPI Seriia – Radiotekhnika Radioaparatobuduvannia, 2024, Iss. 95, pp. 16–22

UDC 621.396.962

Implementation of Method of Minimizing the Side Lobe Level of Autocorrelation Functions of Signals With Nonlinear Frequency Modulation

Kostyria O. O., Hryzo A. A., Khizhnyak I. A., Fedorov A. V., Lukianchykov A. A.

Ivan Kozhedub Kharkiv National Air Force University, Kharkiv, Ukraine

E-mail: *oleksandr.kostyria@nure.ua*

An important problem that is solved during the creation of new and modernization of existing radar equipment is to ensure the maximum range of detection of air targets, which requires increasing the radiated power while maintaining the required range resolution. Since the generating devices, which are now widely used as semiconductor elements, have limited peak power, the required energy is emitted by increasing the duration of the sensing radio pulse, and the requirements for resolution are met by using so-called complex signals, the product of the spectrum width of which and their duration (signal base) is greater than one. One of the types of complex signals is multifragment signals with nonlinear frequency modulation, which, unlike the well-known linear frequency modulated signals, have a significantly lower peak side lobes level of autocorrelation functions, but the value of this level depends significantly on the frequency and time parameters of the signal. Finding parameters that minimize the side lobes level of the autocorrelation function of nonlinear frequency modulated signals, which include fragments with linear frequency modulation, is an important scientific and technical problem, the solution of which is the subject of this article. The peculiarity of considering this issue is that, in contrast to the previously proposed implementation of the method of minimizing the side lobes level for mathematical models with a current time change, the paper develops models of shifted time, that is, when the time count of each subsequent signal fragment is shifted to zero. The first section of the paper analyzes the known publications, which shows that the method of minimizing the side lobes level of correlation functions has not been considered before for mathematical models of the shifted. Given this circumstance, the second section of the paper formulates the research objectives. The theoretical justification of a new variant of the proposed method by developing mathematical time-shifted models for two- and three-fragment nonlinear frequency-modulated signals, as well as the modeling results, are presented in Section 3. In further research, it is planned to develop an algorithm for optimizing the time-frequency parameters of signals with nonlinear frequency modulation based on mathematical models of current and shifted time.

Keywords: nonlinear frequency modulation; autocorrelation function; minimization the side lobes level

DOI: 10.20535/RADAP.2024.95.16-22

Introduction

Observation radar stations for airspace control should provide the maximum possible range of distance measurement to location objects, which is determined by the minimum and maximum range of target detection. The determining parameter for the minimum range is the duration of the sensing signal, for the duration of which the receiving device is blanking. The maximum range at a fixed peak transmitter power is also determined by the duration of the sensing signal. Such contradictory requirements led to the use of signals with intra-pulse modulation (IPM), for which the product B of the frequency bandwidth Δf_S by signal duration T_S (signal base) $B = \Delta f_S T_S > 1$. It is in proportion to this value that the signal duration at the output of the coordinated processing device decreases. This makes it possible to obtain the required value of the resolution from the range when using a signal of long duration and is ensured by using complex signals with IPM frequency or signal phase [1–6].

The use of complex signals allows us to obtain a wider spectral width, which determines the range resolution while keeping the signal duration unchanged. Complex signals, which include linear-frequency modulated (LFM) signals, are widely used, but their disadvantage is a significant peak side lobe level (PSLL, SLL) of the autocorrelation function (ACF). For LFM signals, the PSLL varies little depending on their parameters and is not lower than -13,5 dB. To reduce it, additional measures are taken, namely, weight processing (WP) of the signal in the radio receiving device [7–9] and/or nonlinear frequency modulation (NLFM) of the sensing signal [6, 10–20].

The use of NLFM signals can significantly reduce the PSLL of ACF [6, 10–20], but this result largely depends on the value of their frequency-temporal parameters. In [21], a method was proposed to minimize the PSLL of NLFM signals based on parameter optimization by providing an integer number of radio oscillation periods for each LFM fragment. To describe the signals, a mathematical model (MM) of the current time is used [22–24], while such a method has not been implemented for the MM of the shifted time [25–27]. It is proposed to extend this method to the MM of NLFM signals in shifted time.

1 Analysis of research and publications

The use of frequency and phase IPM of radar signals has been substantiated in detail in a large number of works, for example, [4–6], which outline the fundamental principles of synthesizing probing radar signals. Publication [6] focuses specifically on the problem of maintaining a given range resolution and the issue of joint measurement of the range and speed of location objects when using complex signals. Among the complex signals, the most widely used are the LFM signals, due to the relative simplicity of implementing systems for their formation and processing. However, with the advent of these signals, the problem of reducing the PSLL of their ACF has arisen; this issue has long been under the close attention of scientists, and many others have been devoted to it [12, 13, 16, 18–21].

The authors of [28] propose to reduce the PSLL by changing the law of signal modulation to the NLFM, which consists of a random sequence of LFM fragments, emphasizing that this mitigates the effect of masking the nearest targets by the side lobes of a more powerful compressed signal and allows increasing the useful dynamic range of the radio receiving device.

In [25], it is noted that the magnitude of the PSLL can be reduced by using the NLFM for signals with a base size $B > 100$.

The authors of [6, 10–27] consider NLFM signals of various types, but a single physical principle is used to reduce the PSLL: in the lower and upper frequency regions, the spectral power density of the signal decreases, which results in spectrum rounding, which is equivalent to the WP in the time plane.

NLFM signals with a bell-shaped spectrum, which are considered in [29], provide a significant reduction in the PSLL, but the spectrum of such a signal has an excessive width that does not match the bandwidth of the transmitting and receiving path. Another disadvantage of NLFM signals is the expansion of the main lobe (ML) of the ACF, as a result of which the radar's resolution from the range deteriorates [19–22, 25–27].

In [20, 21], new MMs for NLFM signals and a method for optimizing their parameters were proposed, which was implemented for the case of the current time change. Analogous MMs for time-shifted operation are not considered in the known literature.

2 Formulation of the research task

The aim of this work is to develop a variant of the method of searching for sets of frequency parameters of NLFM signals that ensure minimization of the PSLL of two- and three-fragment NLFM signals. The method is applied to signals described by the time-shifted MM. Minimization of the PSLL is achieved by modifying the values of the frequency modulation rate (FMR) in such a way as to provide an integer number of periods of radio frequency oscillations for each LFM fragment.

3 Materials and methods

3.1 Implementation of the method for reducing the PSLL of ACF NLFM signals based on time-shifted MM

As an initial one, we apply the time-shifted MM of the NLFM signal consisting of three LFM fragments [13] for the case of an increasing law of frequency modulation, in which, by analogy with [20], compensating phase components are introduced. In the formation of such a signal, a negative shift of the initial time for each subsequent LFM fragment by the duration of the previous ones is applied. This mathematical technique automatically compensates for frequency jumps at the junctions of the NLFM signal fragments. The remaining phase jumps are eliminated by introducing the corresponding compensating components for the second and then the third LFM fragments:

$$\varphi_n(t) = \begin{cases} 2\pi\left[f_0 t + \dfrac{\beta_1}{2}t^2\right], \quad 0 \le t \le T_1; \\ 2\pi\left[(f_0 + \beta_1 T_1)(t - T_1) + \beta_2\left(\dfrac{t^2}{2} - T_1 t\right)\right] + \delta\varphi_{12}, \quad T_1 \le t \le T_2; \\ 2\pi\left[(f_0 + \beta_1 T_1 + \beta_2 T_2)(t - T_{12}) + \beta_3\left(\dfrac{t^2}{2} - T_{12} t\right)\right] + \delta\varphi_{23}, \quad T_{12} \le t \le T_S; \end{cases} \tag{1}$$

where $\beta_i = \frac{\Delta f_i}{T_i}$ is the frequency deviation of the i-th ($i = 1, 2, 3$) LFM fragment;

T_i is the duration of the i-th LFM fragment;

Δf_i is the frequency deviation of the i-th LFM fragment;

$T_{12} = T_1 + T_2$ is the total duration of the first and second LFM fragments;

$T_S = T_1 + T_2 + T_3$ is the total duration of all the LFM fragments.

In expression (1), these phase jumps are compensated for by the phase components $\delta\varphi_{12}$ and $\delta\varphi_{23}$. The values of these components are calculated by the following expressions:

$$\delta\varphi_{12} = \pi T_1^2(\beta_2 + \beta_1); \tag{2}$$

$$\delta\varphi_{23} = \pi[T_1^2(\beta_3 + \beta_1) + T_2^2(\beta_3 + \beta_2)]. \tag{3}$$

In [21], a method was proposed to reduce the PSLL of ACF NLFM signals by eliminating one of the causes of phase jumps, which is based on modifying the values of the FMR in each of the signal sections in such a way as to obtain an integer number of periods of radio frequency oscillations in each LFM fragment. Let's apply this approach to the time-shifted MM (1), for which we define an integer number of periods of radio frequency oscillations N_i for each of the LFM fragments of the NLFM signal (1), the symbol].[means the operation of rounding to the nearest larger integer:

$$N_i = \left]\frac{\Psi_i}{2\pi}\right[. \tag{4}$$

Corresponding value of the total phase advance Ψ_i for the first LFM fragment:

$$\Psi_1 = 2\pi\left(f_0 T_1 + \frac{\beta_1}{2}T_1^2\right) = 2\pi N_1 \tag{5}$$

and, after applying operation (4), we find the adjusted value of the FMR $\tilde{\beta}_1$ by solving (5) with respect to it:

$$\tilde{\beta}_1 = \frac{2\,(N_1 - f_0 T_1)}{T_1^2}. \tag{6}$$

The same is true for the second LFM fragment:

$$\Psi_2 = 2\pi(f_0 - \tilde{\beta}_1 T_1)(t - T_1) + \beta_2\left(\frac{t^2}{2} - T_1 t\right) = 2\pi N_2,$$

where : (7)

$$\tilde{\beta}_2 = \frac{N_2 - (f_0 - \tilde{\beta}_1 T_1)(T_2 - T_1)}{\frac{T_2^2}{2} - T_2 T_1}.$$

Accordingly, for the third LFM fragment, we obtain:

$$\Psi_3 = 2\pi\left((f_0 + \tilde{\beta}_1 T_1 + \tilde{\beta}_2 T_2)(t - T_{12}) + \beta_3\left(\frac{t^2}{2} - T_{12} t\right)\right) = 2\pi N_3;$$

$$\tilde{\beta}_3 = \frac{N_3 - (f_0 - \tilde{\beta}_1 T_1 - \tilde{\beta}_2 T_2)(T_S - T_{12})}{\frac{T_S^2}{2} - T_S T_{12}}. \tag{8}$$

It should be emphasized that in order to find each subsequent corrected FMR value, it is necessary to use the corresponding corrected values already obtained for the previous fragments.

Despite the fact that the final phases of the LFM fragments have a value of 2π, the initial phases of the second and third fragments in the vast majority of cases are not equal to zero. The phase jump at the beginning of these fragments is caused by a change in the value of the FMR at this point in time, and therefore must be compensated. That is, the compensating components (2), (3) in the new MM remain with the change of the initial values of the FMR to the modified ones:

$$\delta\tilde{\varphi}_{12} = \pi T_1^2\left(\tilde{\beta}_2 + \tilde{\beta}_1\right); \tag{9}$$

$$\delta\tilde{\varphi}_{23} = \pi\left(T_1^2\left(\tilde{\beta}_3 + \tilde{\beta}_1\right) + T_2^2\left(\tilde{\beta}_3 + \tilde{\beta}_2\right)\right). \tag{10}$$

Using (6)-(10), we obtain the MM of a three-fragment NLFM signal in shifted time, which provides an integer number of periods of radio oscillations of each of the LFM fragments:

$$\varphi_n(t) = \begin{cases} 2\pi\left[f_0 t + \dfrac{\tilde{\beta}_1}{2}t^2\right], & 0 \le t \le T_1; \\ 2\pi\left[(f_0 + \tilde{\beta}_1 T_1)(t - T_1) + \tilde{\beta}_2\left(\dfrac{t^2}{2} - T_1 t\right)\right] + \delta\tilde{\varphi}_{12}, & T_1 \le t \le T_2; \\ 2\pi\left[(f_0 + \tilde{\beta}_1 T_1 + \tilde{\beta}_2 T_2)(t - T_{12}) + \tilde{\beta}_3\left(\dfrac{t^2}{2} - T_{12} t\right)\right] + \delta\tilde{\varphi}_{23}, & T_{12} \le t \le T_S. \end{cases} \tag{11}$$

It should be noted that when applying the modified values of the FMR, the obtained updated values of the fragment frequency deviation may differ from the original ones, that is, in the case of $\tilde{\beta}_i \neq \beta_i$, we have respectively $\Delta\tilde{f}_i \neq \Delta f_i$. The results of testing the performance of the developed MM are presented in the next subsection.

3.2 Results of mathematical modeling

Mathematical modeling was performed in accordance with (1) and (11). For two-fragment NLFM

signals, the first two expressions of these MMs were used, the results are given in Table 1, for three-fragment signals – in Table 2. The fragment durations remained unchanged for both models.

A comparative analysis of the data in Table 1 shows a decrease in the PSLL when using MM [11]. The achieved reduction of the PSLL is within 1 dB. Regarding the rate of decay of the side lobe level (SLL), no significant advantages are observed for the proposed MM (11), as it should be, since MM (11) is actually a special case of MM (1). The deviations of the SLL decay rate with respect to MM (1) range from -1 dB/dec to 3 dB/dec for the variants shown in Table 1. The values given in parentheses correspond to MM (11).

The data in Table 2 indicate the feasibility of using MM [11]. Due to the provision of a whole number of periods of radiofrequency oscillations on each of the LFM fragments, a steady decrease in the PSLL is observed, the maximum value of which is 3.5 dB (variant No. 1).

Table 1 Results of modeling two-fragment NLFM signals

№ in order	T_1, μs	T_2, μs	Δf_1, kHz	Δf_2, kHz	PSLL, dB	Decay rate of SLL, dB/dec
1.	30,0	150,0	200,0 (200,0)	450,0 (453,3)	-18,01 (-18,09)	20,0 (21,0)
2.	35,0	200,0	300,0 (285,7)	700,0 (698,6)	-17,82 (-18,32)	23,0 (22,5)
3.	40,0	200,0	100,0 (100,0)	220,0 (222,22)	-18,00 (-18,14)	21,0 (21,0)
4.	45,0	220,0	100,0 (88,8)	200,0 (204,0)	-17,24 (-18,22)	21,0 (19,0)
5.	50,0	280,0	100,0 (80,0)	200,0 (218,6)	-16,85 (-17,17)	21,0 (24,0)

Table 2 Results of modeling three-fragment NLFM signals

№ in order	T_1, μs	T_2, μs	T_3, μs	Δf_1, kHz	Δf_2, kHz	Δf_3, kHz	PSLL, dB	Decay rate of SLL, dB/dec
1.	20,0	80,0	20,0	80,0 (100,0)	200,0 (200,0)	95,0 (100,0)	-20,22 (-23,52)	14,0 (16,5)
2.	20,0	100,0	20,0	80,0 (100,0)	200,0 (200,0)	90,0 (100,0)	-22,06 (-23,07)	18,0 (18,0)
3.	30,0	150,0	30,0	100,0 (66,667)	200,0 (186,67)	100,0 (93,33)	-20,97 (-22,85)	21,0 (20,0)
4.	30,0	150,0	30,0	150,0 (133,33)	300,0 (306,67)	150,0 (120,00)	-19,95 (-21,80)	22,0 (21,0)
5.	50,0	250,0	50,0	150,0 (160)	350,0 (352,0)	150,0 (136,00)	-20,88 (-21,23)	22,0 (22,0)

If the modified input values from (11) are substituted into (1), the final result will be identical, since (11) is a special case of (1) and complements the set of possible values of its frequency parameters.

According to Tables 1 and 2, we determined the ratio of the duration of the LFM fragments and their frequency deviations, which ensures the performance of (1) and (11). The results are summarized in Table 3. The results of the calculations are given in relation to the parameters of the first LFM fragment.

Table 3 Correlation between the duration and frequency deviations of the LFM fragments

Ratio of fragment duration			
2 fragments		3 fragments	
from 1:5	to 1:5,7	from 1:4:1	to 1:5:1
Ratio of frequency deviations			
Mathematical model (1)			
from 1:2	to 1:2,5	from 1:2:1	to 1:2,5:1
Mathematical model (11)			
from 1:2,2	to 1:2,7	from 1:2:1	to 1:2,9:1,4

The analysis of the results in Table 3 shows that when the proposed method of minimizing the PSLL for a two-fragment NLFM signal (MM (11)) is applied, the range of change in the frequency deviations of the LFM fragments remains unchanged but has shifted by 10%, that is, the range of change in this parameter has expanded by this value. For a three-fragment signal, in the case of MM (11), compared to MM (1), there is an expansion of the range of change in frequency deviation by 20% for the component of the second LFM fragment and by 40% for the component of the third.

Figures 1 and 2 show the results of modeling the two- and three-fragment signals that provided the lowest value of the PSLL – parameter sets No. 2 of Table 1 and No. 1 of Table 2.

The graphs of the fragment frequency changes (Fig. 1a, Fig. 2a) correspond to the specified frequency parameters of the NLFM signals. The spectra of these signals are shown in Fig. 1b and Fig. 2b, they demonstrate smooth transitions between fragments and the absence of pulsations on the slopes, which indicates full compensation of instantaneous phase jumps in the resulting signals. The corresponding ACF signals (Fig. 1c and Fig. 2c) have smooth slopes and a uniform change in the side lobes (SL) ripple frequency, which also indicates the absence of phase distortion of the signals.

Conclusions

The result of the performed research is the development of a variant of the practical implementation of the method of searching for frequency parameters for MM two- and three-fragment NLFM signals, which ensures a decrease in the PSLL of their ACF.

The novelty of our results lies in the extension of the known method of compensating for instantaneous phase jumps to the time-shifted MM, that is, when the time scale for each subsequent fragment is shifted by the duration of the previous ones. The application of the proposed MM provides an expansion of the range of input values of frequency parameters and facilitates their detection. The ratio of deviations in the frequency and duration of the LFM fragments, which ensures the efficiency of the proposed MM, was determined experimentally.

The obtained experimental data confirmed the possibility of reducing the PSLL when applying the proposed method for a two-fragment NLFM signal within 1 dB, and for a three-fragment signal - up to 3.5 dB.

The practical significance of the obtained results is to expand the possible variants of NLFM signals by changing the frequency parameters that meet the requirements of users. With regard to the field of radar, this will ensure the adaptation of the air target detection mode to the conditions of the signal-interference environment.

The obtained values of the sets of PSLL signal parameters can be considered as an initial set for further optimization, for example, using evolutionary algorithms. This approach is expected to reduce the number of algorithm iterations.

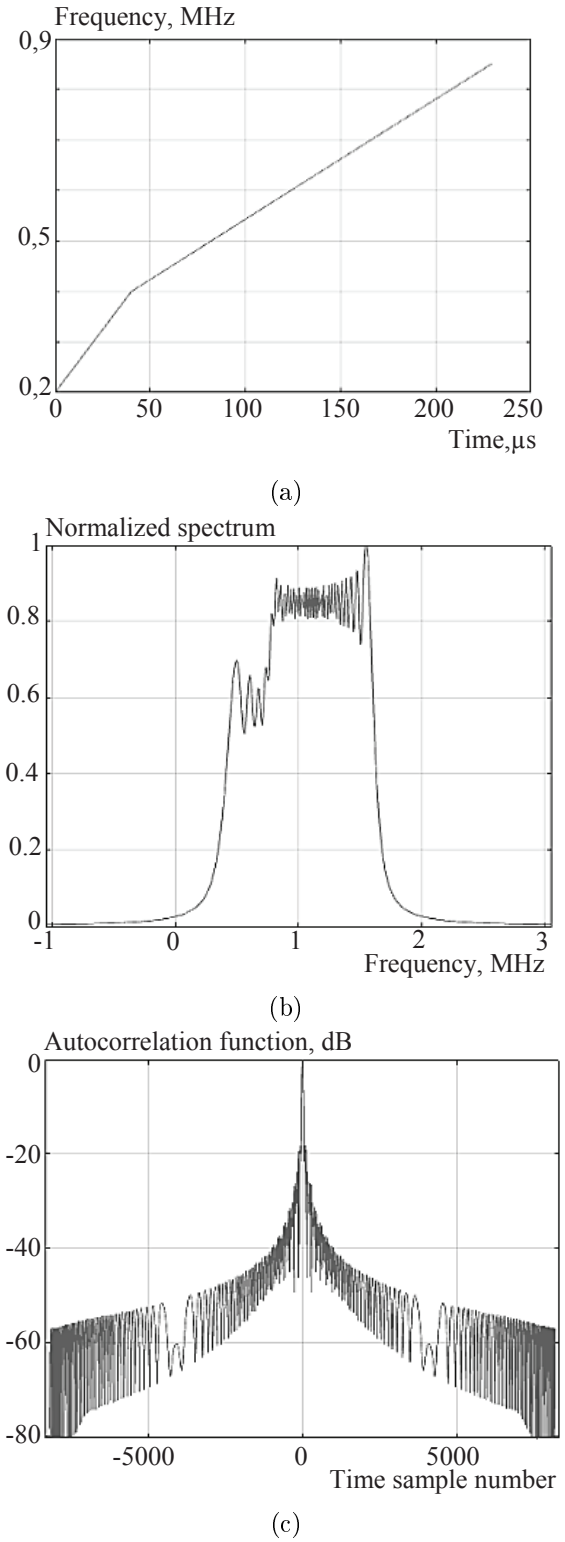

Fig. 1. Graph of changes in the instantaneous time-total (a), spectrum (b), ACF (c) of the two-frequency NLFM signal

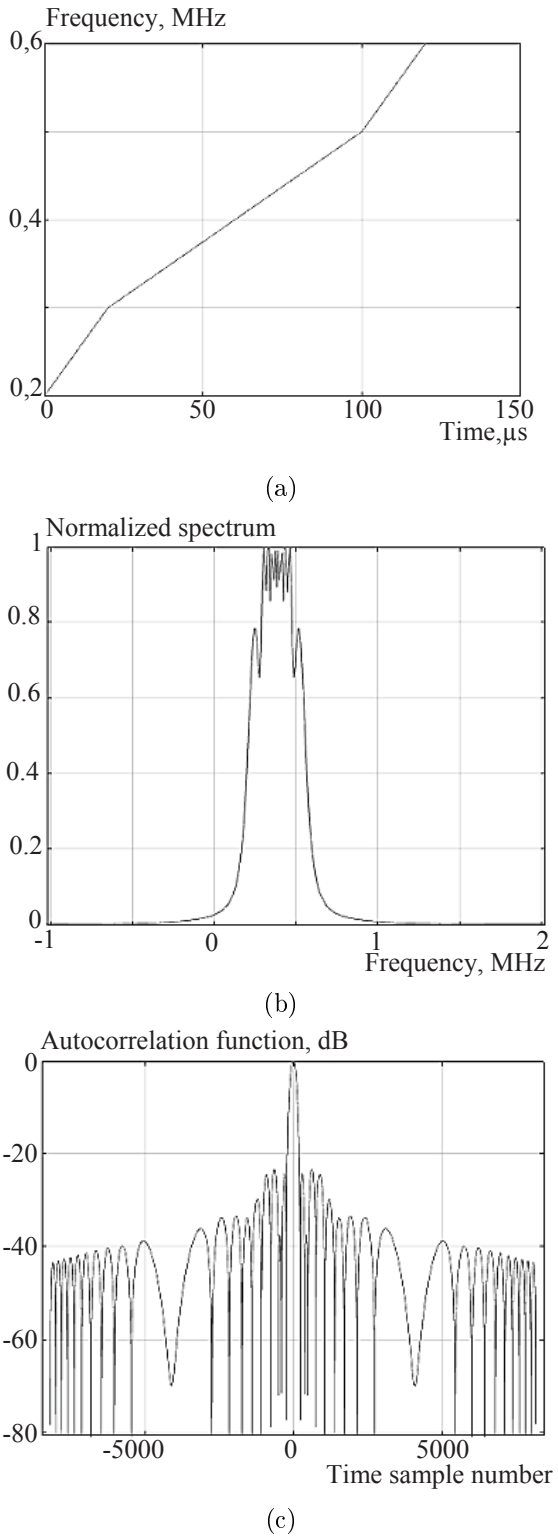

Fig. 2. Graph of instantaneous frequency change (a), spectrum (b), ACF (c) of a three-fragment NLFM signal

References

[1] Skolnik M. I. (1981) *Introduction to Radar Systems*. Second Edition. Singapore: McGraw-Hill Book Co., 581 p.

[2] Richards M. A., Scheer J. A., Holm W. A. (2010) *Principles of modern radar*, Vol. I: Basic Principles, Chelsea: Sheridan Books, Inc., 962 p.

[3] Meikle H. (2008) *Modern Radar Systems*. Second Edition. Norwood: Artech House, Inc, 701 p.

[4] Kwok Tom, Kenneth Ranney (2020) Survey of Methodology and Features for Radar Waveform Modulation Classification. *CCDC Army Research Laboratory*, Sensors and Electron Devices Directorate, ARL-TR-9062, 42 p.

[5] Levanon N., and Mozeson E. (2004) *Radar Signals*. Wiley IEEE Press.

[6] Cook C. E., and Bernfeld M. (1993) *Radar Signals: An Introduction to Theory and Appli-cation*. Artech House, 552 p.

[7] Heinzel G., Rüdiger A., and Schilling R. (2002) Spectrum and spectral density estimation by the Discrete Fourier transform (DFT), including a comprehensive list of window functions and some new flat-top windows. Technical Report. *Max-Planck-Institut für Gravitationsphysik (Albert-Einstein-Institut)*, Germany, 84 p.

[8] Valli N. A., Rani D. E., Kavitha C. (2019) Windows for Reduction of ACF Sidelobes of Pseudo-NLFM Signal. *International Journal of Scientific & Technology Research*, Vol. 8, Iss. 10, pp. 2155-2161.

[9] Doerry A. W. (2017) Catalog of Window Taper Functions for Sidelobe Control. Technical Report SAND2017-4042. *U.S. Department of Energy Office of Scientific and Technical Information*, 208 p. doi: 10.2172/1365510.

[10] Swiercz E., Janczak D., and Konopko K. (2022) Estimation and Classification of NLFM Signals Based on the Time-Chirp Representation. *Sensors*, Vol. 22, 8104. doi: 10.3390/s22218104.

[11] Alphonse S., Williamson G. A. (2014) Novel radar signal models using nonlinear frequency modulation. *22nd European Signal Processing Conference (EUSIPCO)*, doi:10.5281/ZENODO.44184.

[12] Song Chen, et al. (2022) A Novel Jamming Method against SAR Using Nonlinear Frequency Modulation Waveform with Very High Sidelobes. *Remote Sensing*, Vol. 14, Iss. 21, 5370. doi:10.3390/rs14215370.

[13] Chukka A. and Krishna B. (2022) Peak Side Lobe Reduction analysis of NLFM and Improved NLFM Radar signal. *Aiub Journal of Science and Engineering (AJSE)*, Vol. 21, Iss. 2, pp. 125-131. doi: 10.53799/ajse.v21i2.440.

[14] Fan Z., Meng H. (2020) Coded excitation with Nonlinear Frequency Modulation Carrier in Ultrasound Imaging System. *IEEE Far East NDT New Technology & Application Forum (FENDT)*. doi:10.1109/FENDT50467.2020.9337517.

[15] Zhao Y., et al. (2020) Non-continuous piecewise nonlinear frequency modulation pulse with variable subpulse duration in a MIMO SAR Radar System. *Remote Sensing Letters*, Vol. 11(3), pp. 283-292. doi:10.1080/2150704X.2019.1711237.

[16] Jin G. et al. (2019) An Advanced Nonlinear Frequency Modulation Waveform for Radar Imaging With Low Sidelobe. *IEEE Transactions on Geosciences and Remote Sensing*, Vol. 57, Iss. 8, pp. 6155–6168. doi:10.1109/TGRS.2019.2904627.

[17] Saleh M., Omar S.-M., Grivel E., Legrand P. (2021) A Variable Chirp Rate Stepped Frequency Linear Frequency Modulation Waveform Designed to Approximate Wideband Non-Linear Radar Waveforms. *Digital Signal Processing*, Vol. 109. doi: 10.1016/j.dsp.2020.102884.

[18] Xu, Z.; Wang, X.; Wang, Y. (2022) Nonlinear Frequency-Modulated Waveforms Modeling and Optimization for Radar Applications. *Mathematics*, Vol. 10(21), 3939, pp. 1-11. doi: 10.3390/math10213939.

[19] Kavitha C., Valli N. A., Dasari M. (2020) Optimization of two-stage NLFM signal using Heuristic approach. *Indian Journal of Science and Technology (INDJST)*, Vol. 13(44), pp. 4465-4473. doi:10.17485/IJST/v13i44.1841.

[20] Kostyria O. O., Hryzo A. A., Dodukh O. M., Nariezhnii O. P. & Fedorov, A. V. (2023) Mathematical model of the current time for three-fragment radar signal with nonlinear frequency modulation. *Radio Electronics, Computer Science, Control*, Vol. 3(63), pp. 17-26. doi: 10.15588/1607-3274-2023-3-2.

[21] Kostyria O. O., Hryzo A. A., Dodukh O. M., Lisohorskyi B. A., & Lukianchykov A. A. (2023) Method of minimization sidelobes level autocorrelation functions of signals with non-linear frequency modulation. *Radio Electronics, Computer Science, Control*, Vol. 4(67), pp. 39-48. doi: 10.15588/1607-3274-2023-4-4.

[22] Prakash B. L., Sajitha G., and Rajeswari K. R. (2016) Generation of Random NLFM Signals for Radars and Sonars and their Ambiguity Studies. *Indian Journal of Science and Technology*, Vol. 9, Iss. 29, pp. 1-7. doi:10.17485/ijst/2016/v9i29/93653.

[23] Kurdzo J. M., et al. (2019) A Neural Network Approach for Waveform Generation and Selection with Multi-Mission Radar. *IEEE Radar Conference*, pp. 1-6. doi:10.1109/RADAR.2019.8835803.

[24] Bayındır C. (2015) A Novel Nonlinear Frequency Modulated Chirp Signal for Synthetic Aperture Radar and Sonar Imaging. *Journal of Naval Science and Engineering*, Vol. 11, No. 1, pp.68-81.

[25] Valli N. A., Rani D. E., Kavitha C. (2019) Modified Radar Signal Model using NLFM. *International Journal of Recent Technology and Engineering (IJRTE)*, Vol. 8, Iss. 2S3, pp. 513-516. doi: 10.35940/ijrte.B1091.0782S319.

[26] Jeevanmai R., Rani N. D. (2016) Side lobe Reduction using Frequency Modulated Pulse Compression Techniques in Radar. *International Journal of Latest Trends in Engineering and Technology*, Vol. 7, Iss. 3, pp. 171-179. doi: 10.21172/1.73.524.

[27] Adithyavalli N., Rani D. E., Kavitha C. (2019) An Algorithm for Computing Side Lobe Values of a Designed NLFM function. *International Journal of Advanced Trends in Computer Science and Engineering*, Vol. 8(4), pp. 1026-103. doi:10.30534/ijatcse/2019/07842019.

[28] Galati G., Pavan G., and De Palo F. (2017). Chirp Signals and Noisy Waveforms for Solid-State Surveillance Radars. *Aerospace*, Vol. 4(1), 15, 14 p. doi:10.3390/aerospace4010015.

[29] Leśnik C. (2009) Nonlinear Frequency Modulated Signal Design. *Acta Physica Polonica A*, Optical and Acoustical Methods in Science and Technology, Vol. 116, No. 3, pp. 351-354. doi:10.12693/APhysPolA.116.351.

Реалізація методу мінімізації рівня бічних пелюсток автокореляційних функцій сигналів з нелінійною частотною модуляцією

Костиря О. О., Гризо А. А., Хижняк І. А., Федоров А. В., Лук'янчиков А. А.

Важливою проблемою, яка вирішується під час створення нової та модернізації існуючої радіолокаційної техніки, є забезпечення максимальної дальності виявлення повітряних цілей, для чого необхідно збільшувати випромінювану потужність зі збереженням потрібної розрізнювальної здатності з дальності. Оскільки генераторні прилади, у якості яких зараз широко застосовуються напівпровідникові елементи, мають обмежену пікову потужність, випромінювання необхідної енергії здійснюється за рахунок збільшення тривалості зондувального радіоімпульсу, а вимоги з розрізнювальної здатності виконуються за рахунок використання так званих складних сигналів, добуток ширини спектру яких на їхню тривалість (база сигналу) більше одиниці.

Одним з різновидів складних сигналів є багатофрагментні сигнали з нелінійною частотною модуляцією, які на відміну від широко відомих лінійно-частотно модульованих сигналів мають суттєво нижчий максимальний рівень бічних пелюсток автокореляційних функцій, однак значення цього рівня суттєво залежить від заданих частотно-часових параметрів сигналу. Знаходження параметрів, які забезпечують мінімізацію рівня бічних пелюсток автокореляційних функції нелінійно-частотно модульованих сигналів, до складу яких входять фрагменти з лінійною модуляцією частоти, є важливою науково-технічною задачею, вирішенню якої присвячено дану статтю. Особливість розгляду зазначеного питання полягає у тому, що на відміну від раніше запропонованої реалізації методу мінімізації рівня бічних пелюсток для математичних моделей з поточною зміною часу у даній статті розробляються моделі зсунутого часу, тобто коли відлік часу кожного наступного фрагменту сигналу зсувається на нульову відмітку. У першому розділі статті проведено аналіз відомих публікацій, який показує, що для математичних моделей зсунутого часу спосіб мінімізації рівня бічних пелюсток функцій кореляції раніше не розглядався. З огляду на дану обставину у другому розділі роботи сформульовано завдання дослідження. Теоретичне обґрунтування нового варіанту реалізації запропонованого методу шляхом розробки математичних моделей зсунутого часу для дво- та трифрагментних нелінійно-частотно модульованих сигналів, а також результати моделювання наведено у третьому розділі роботи. У подальших дослідженнях планується розробити алгоритм оптимізації частотно-часових параметрів сигналів з нелінійною частотною модуляцією на основі математичних моделей поточного та зсунутого часу.

Ключові слова: нелінійна частотна модуляція; автокореляційна функція; мінімізація рівня бічних пелюсток